https://doi.org/10.31436/iiumej.v27i3.4517

Repeated Loading Behavior of CFRP-Strengthened Continuous RC Beams: Experimental Investigation, Finite Element Analysis, and Predictive Modeling

Zeinab R. Moubarek [1*], **Ehab M. Lotfy**[2], **Manar A. Ahmed** [2], **Erfan A. Latef**[2], **Ezzaat A. Sallam**[3]

[1]*Dept. of Civil Engineering, Obour High Institute for Engineering and Technology, Cairo, Egypt*
[2]*Dept. of Civil Engineering, Faculty of Engineering, Suez Canal University, Egypt*
[3]*Dept. of Civil Engineering, Faculty of Engineering, Port Said University, Egypt*

**Corresponding author: zreda1251@gmail.com*

(Received: 11 June 2026; Accepted: 1 July 2026; Published online: 11 September 2026)

ABSTRACT: This study investigates the repeated-loading performance and moment redistribution of continuous reinforced concrete (RC) T-beams strengthened with carbon fiber-reinforced polymer (CFRP) using a combined experimental and numerical approach. The experimental part studies the effect of reinforcement percentage and the CFRP strengthening configuration, while the FE model validates the effect of compressive strength of concrete, ratio of span to depth, CFRP reinforcement percentage, CFRP length percentage, loading frequency, and yield strength of steel on the behavior of the structure under repeated loadings. Five half-scale two-span RC T-beams having different reinforcement percentages and CFRP configurations were experimentally tested under repeated loading. CFRP strengthening increased load capacity by up to 16% and improved ductility, energy dissipation, stiffness degradation, and crack distribution; noticeable benefits were observed with the hybrid-strengthening system. The maximum ductility ratio increased from 2.7 in the control beam to 4.8 in the reinforced beams. In summary, the conflict between the stiffening effect and rotational capacity was found to be the key factor controlling the moment redistribution process. Three-dimensional non-linear finite element (FE) modeling was performed, which showed good agreement with the experimentally obtained load-displacement curve, stiffness degradation, strain evolution, and cracking pattern trends. Utilizing the validated FE database, a predictive model based on multiple regression analysis with a power-law multiplicative formulation was constructed.

ABSTRAK: Kajian ini menyiasat prestasi berterusan rasuk T konkrit bertetulang (RC) yang diperkukuh menggunakan polimer gentian karbon (CFRP) di bawah beban berulang, serta tingkah laku pengagihan semula momen melalui gabungan pendekatan eksperimen dan numerik. Pengaruh nisbah tetulang dan konfigurasi pengukuhan CFRP dinilai melalui eksperimen. Manakala model unsur terhingga (FE) digunakan bagi mengesah kesan kekuatan mampatan konkrit, nisbah rentang kepada kedalaman, nisbah tetulang CFRP, nisbah panjang CFRP, frekuensi pembebanan, dan kekuatan luluh keluli terhadap tindak balas struktur di bawah pembebanan berulang. Lima rasuk T (RC dua bentang) berskala separuh dengan nisbah tetulang dan konfigurasi CFRP berbeza telah diuji secara eksperimen di bawah beban berulang. Penggunaan pengukuhan CFRP meningkatkan kapasiti beban sehingga 16% serta menambah baik kemuluran, pelesapan tenaga, degradasi kekakuan, dan taburan retakan, dengan prestasi terbaik dicapai pada konfigurasi pengukuhan hibrid. Nilai maksimum nisbah kemuluran meningkat daripada 2.7 bagi rasuk kawalan kepada 4.8 bagi rasuk pengukuhan. Secara keseluruhan, dapatan menunjukkan bahawa keseimbangan antara peningkatan kekakuan dan kapasiti putaran merupakan faktor utama mengawal proses pengagihan semula momen. Pemodelan tiga dimensi unsur terhingga (FE) tak linear menunjukkan padanan baik dengan dapatan eksperimen dari segi lengkung beban–sesaran, degradasi kekakuan, evolusi regangan, dan corak keretakan. Berdasarkan pangkalan data FE yang telah disahkan, satu model ramalan berasaskan analisis regresi berganda menggunakan formulasi hukum kuasa multiplikatif telah dibangunkan.

KEYWORDS: *Repeated loading, Continuous RC beam, CFRP strengthening, Moment redistribution, Finite element modeling.*

1. INTRODUCTION

Continuous RC beams are commonly used because of their structural redundancy, economical use of materials, and ability to redistribute forces [1, 2]. Unlike simple beams, continuous beams allow moment redistribution due to the formation of plastic hinges under repeated or cyclic loading [3, 4]. However, repeated loading induces complex responses associated with stiffness degradation, crack propagation, reinforcement yielding, and progressive damage accumulation, particularly in the negative moment region over intermediate supports where plastic hinges typically develop [5, 6].

Strengthening and retrofitting of the current RC structures have become relevant issues considering the aging of buildings and increased loads on them [7]. One method used for strengthening is carbon fiber reinforced polymer (CFRP) due to its high strength-to-weight ratio, corrosion protection, ease of installation, and lack of geometrical change [8]. Many studies have proved that CFRP strengthening increases the flexural resistance and stiffness of RC beams [9]. Nevertheless, data on the effect of CFRP strengthening on ductility and moment redistribution are lacking, especially for continuous beams, where stiffness compatibility and rotation capacity play a crucial role. Moreover, most previous investigations have focused on simply supported beams under monotonic loading, providing limited insight into the repeated-loading response of continuous systems [10].

Research on CFRP-strengthened continuous reinforced concrete T-beams has been insufficiently investigated because the interaction between the slab and beam significantly influences stiffness distribution, stress transfer, and failure mode [11]. In addition, the interaction between the internal steel reinforcement and externally bonded CFRP, along with the joint effect of structural and strengthening parameters, has not been sufficiently studied [12, 13]. This makes the analysis of strengthened continuous beams more complicated than that of simply supported beams and requires further investigation that accounts for strength enhancement, deformation capacity, and moment redistribution.

In previous investigations of CFRP-strengthened continuous RC beams, most research considered only monotonic loading conditions. Akbarzadeh and Maghsoudi [14] noted that additional CFRP layers increase the load capacity of continuous beams but can decrease their ductility and moment redistribution owing to the increased stiffness. Ashour et al. [15] stated that CFRP strengthening influences the deformation capacity and failure characteristics of continuous beams. El-Ghandour et al. [16] investigated moment redistribution in CFRP-strengthened continuous beams, and Aiello et al. [17] showed that proper strengthening configuration allows good redistribution properties to be maintained. However, this research mainly focused on monotonic loading and did not consider the effects of progressive repeated loading on stiffness, residual deformations, and damage accumulation.

At the same time, most existing investigations under repeated and cyclic loading conditions focused on simply supported beams rather than continuous structures. For example, El-Saikaly and Chaallal [18] and Tanarslan and Altın [19] showed that CFRP strengthening enhances stiffness retention, crack control, and failure resistance under fatigue and cyclic loading; however, increasing the CFRP strengthening degree decreases ductility due to excessive stiffness. Similar results were obtained in repeated-loading investigations by Fathuldeen and Qissab [20] and Wang et al. [21], where load capacity increased with CFRP strengthening, accompanied by a decrease in deformation capacity due to increased structural stiffness. Nevertheless, these studies mainly considered simply supported beams and did not account for the joint influence of repeated loading, moment redistribution, and CFRP strengthening in continuous RC beams.

To fill this knowledge gap, this study will conduct experimental tests combined with verified non-linear finite element (FE) analysis to investigate the repeated-loading response and moment redistribution of CFRP-strengthened continuous RC T-beams. After verifying the FE model, a series of parametric analyses will be performed to investigate the effect of strengthening arrangement, reinforcement properties, and other factors on load capacity, deformability, stiffness degradation, and redistribution ability in gravity-controlled repeated loading conditions.

The present study provides experimental information on the repeated-loading behavior and moment redistribution of CFRP-strengthened continuous RC T-beams, which have been studied to a relatively lesser extent than simply supported beams. In addition, a non-linear finite element approach will be established and verified to capture the response behavior for conducting parametric studies systematically. Based on the generated database, an empirical equation will be developed to predict load capacity within the tested parameter range. Overall, these contributions will enhance understanding of the interaction between stiffness increase, deformability, and moment redistribution in CFRP-strengthened continuous RC beams under repeated loading conditions.

2. EXPERIMENTAL STUDY

2.1. Specimens and Materials

A series of five half-scale two-span continuous RC T-beams were used to evaluate the influence of the reinforcement ratio and the configuration of the CFRP reinforcement on their behavior. In each specimen, the total length was 4150 mm; the span length was 2000 mm for both spans. The cross section included a web width of 120 mm, an overall depth of 300 mm, and a slab size of 500 mm × 60 mm. The intermediate RC column (150 mm × 200 mm × 150 mm), containing 4 Ø10 longitudinal bars, was utilized to represent the internal support, as shown in Figure 1.

Two reinforcing levels have been examined. In the medium reinforcing series (B-M), 4Ø16 reinforcing bars were used as bottom bars, and 2Ø12 bars were used as top bars. However, the low reinforcing series (B-L) comprised 2Ø12 reinforcing bars as bottom bars and 2Ø10 bars as top bars. All samples had the same transverse reinforcement, consisting of Ø8 plain steel stirrups at 100 mm spacing, and slab reinforcement of 5Ø8/m. All beam specimens were designed following the Egyptian Code of Practice for Design and Construction of Reinforced Concrete Structures (ECP 203-2020) [22] so that flexural failure occurred before shear failure. The yield strength of plain steel stirrups was 240 MPa, which complies with the provisions of ECP 203-2020. The specimen identification includes the beam type (B), reinforcement level (M or L), and strengthening configuration (SL, DL, or DL+D), as summarized in Table 1.

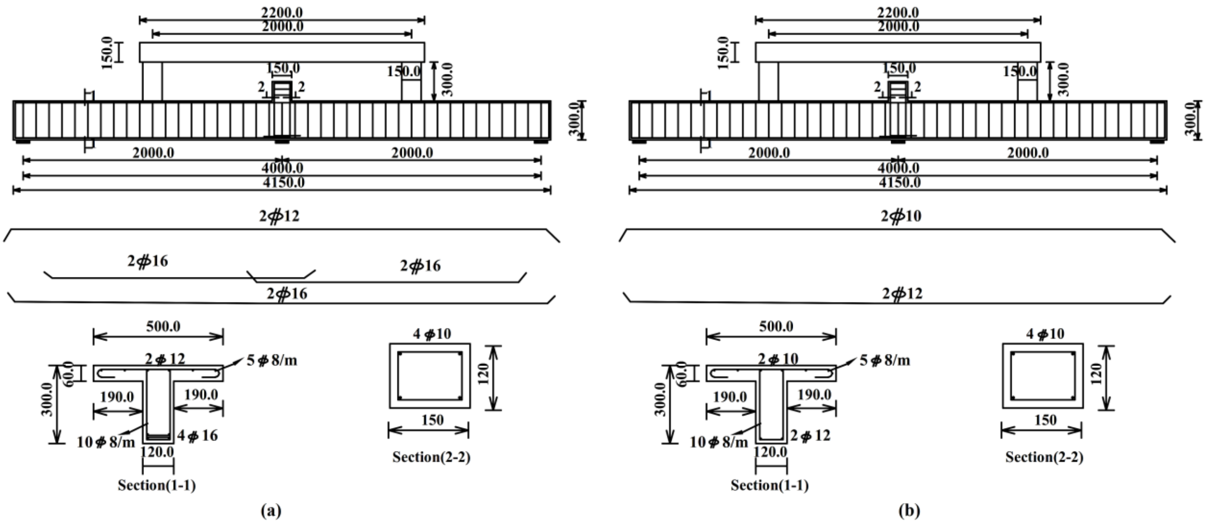

Figure 1. Geometry and reinforcement layout of the tested continuous RC T-beam specimens: (a) medium-reinforcement series (B-M); (b) low-reinforcement series (B-L).

Table 1. Configuration of tested continuous RC T-beam specimens and CFRP strengthening schemes

Specimen ID	Strengthening Scheme	F_{cu} (MPa)	Top Reinforcement (Support)	Bottom Reinforcement (Mid-span)	Stirrups
B-M-CON	Unstrengthened (control)	30	2Ø12	4Ø16	Ø8 @ 100 mm
B-M-SL	SL (single-layer CFRP)	30	2Ø12	4Ø16	Ø8 @ 100 mm
B-L-SL	SL (single-layer CFRP)	30	2Ø10	2Ø12	Ø8 @ 100 mm
B-L-DL	DL (double-layer CFRP)	30	2Ø10	2Ø12	Ø8 @ 100 mm
B-L-(DL+D)	DL+D (hybrid CFRP)	30	2Ø10	2Ø12	Ø8 @ 100 mm

The selected reinforcement layouts were intended to provide different stiffness and deformation behavior and their interaction with CFRP reinforcement under repeated loading. An unstrengthened low-reinforcement control beam was not included because the experimental program was designed to evaluate representative CFRP strengthening configurations rather than to establish a full factorial comparison between reinforcement ratio and strengthening level. Consequently, the individual effects of reinforcement ratio and CFRP strengthening could not be fully isolated experimentally. As a result, direct comparisons between the medium- and low-reinforcement series inherently reflect their combined influence, whereas the low-reinforcement results are interpreted primarily in terms of the incremental effect of increasing the CFRP configuration from single-layer SL to DL and DL+D. To complement the experimental observations, the validated finite element model was subsequently used to vary the reinforcement ratio and CFRP parameters independently, thereby quantifying the individual contribution of each variable.

All specimens were cast with normal-weight concrete with a target compressive strength of 30 MPa. The 28-day strengths of the cube and cylinder specimens were 30 MPa and 25 MPa, respectively, with an elastic modulus of 26 GPa. Mechanical properties of the concrete, steel reinforcement, CFRP sheets, and adhesive are shown in Table 2. Materials testing was carried out according to BS EN 12390-3 [23] for concrete and ASTM A370 [24] for steel.

To maintain uniformity in the properties of the materials used in the test, all beams were cast simultaneously. Instrumentation of the reinforcement cages was done before casting, and the specimens were demolded 24 hours after casting. The specimens were then cured for 28 days under standard conditions, as shown in Figure 2.

Table 2. Material properties of concrete, steel, CFRP, and adhesive

Material	Property	Value
Concrete	Compressive strength, Fcu (MPa)	30
	Cylinder strength (MPa)	25
	Elastic modulus, Ec (GPa)	26
Steel	Yield strength, Fy (MPa)	570
	Elastic modulus, Es (GPa)	200
	Yield strain, εy	0.00285
Plain Steel Stirrups	Yield strength, Fy (MPa)	240
	Elastic modulus (GPa)	195
	Yield strain	0.00123
CFRP	Tensile strength (MPa)	4900
	Elastic modulus (GPa)	252
	Ultimate strain	0.012
	Thickness (mm)	0.164
Adhesive	Tensile strength (MPa)	24.8
	Elastic modulus (GPa)	4.5
	Ultimate strain	0.010

Figure 2. Fabrication stages of the tested continuous RC beam specimens.

2.2. Strengthening Procedure

This paper studied three reinforcement configurations for CFRP strengthening: Single Layer, Double Layer, and Longitudinal-Diagonal. Figure 3 shows these configurations. All reinforced specimens consist of externally bonded CFRP strips, 50 mm wide and 0.164 mm thick per layer, applied to the beam soffit in the span areas. The DL configuration consists of two CFRP layers in the same orientation, whereas DL+D is another CFRP configuration with additional diagonal strips at 45° to control cracks in the most vulnerable area of negative moments.

Before applying CFRP strips, the concrete surfaces were mechanically prepared and cleaned to improve bond effectiveness. Bonding was performed with epoxy resin, and consolidation was achieved using rollers. These configurations were used to investigate the effect of CFRP amount and configuration on the flexural behavior and moment redistribution of continuously reinforced concrete beams under repeated loadings.

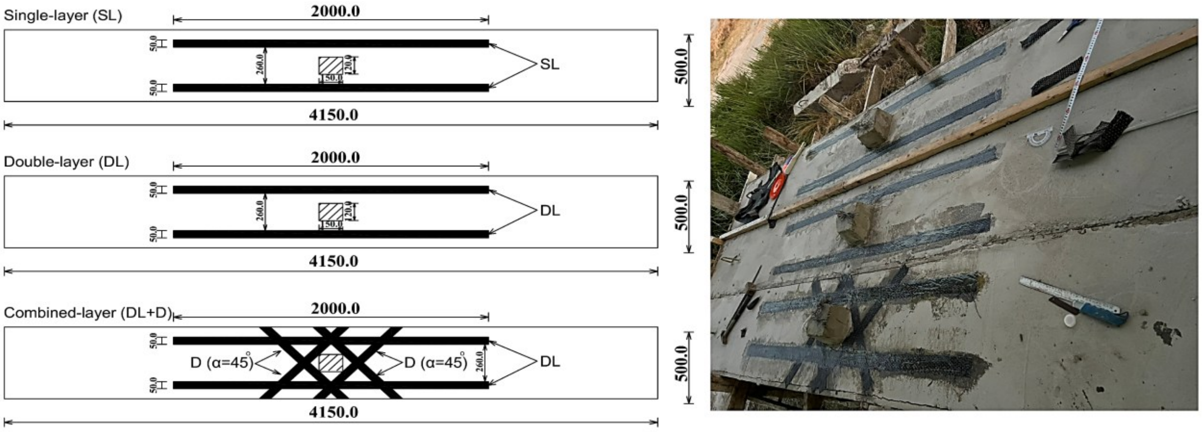

(a) (b)

Figure 3. CFRP strengthening details: (a) strengthening layouts and dimensions; (b) representative strengthened specimen after CFRP application.

2.3. Test Setup and Instrumentation

Each specimen was tested using displacement-controlled repeated loading with a servo-controlled hydraulic actuator mounted on a reaction frame. Continuous RC T-beams were tested at both ends and an intermediate RC column to replicate the condition of the continuous beam. Vertical loading was applied using a steel spreader beam placed above the intermediate support to introduce the negative-moment region. Figure 4 schematically shows the test setup.

Vertical displacement was measured using linear variable differential transformers (LVDTs) located at the midspan of each span and recorded continuously using a computerized data acquisition system. Strain measurements focused on the negative-moment region above the intermediate support. Strain gauges were installed in the top longitudinal reinforcement, the concrete surface, and the CFRP sheets (for strengthened specimens) to investigate the strain distribution and the performance of the strengthening process. Figure 5 indicates the strain gauge positions.

The loading procedure, as shown in Figure 6, followed a standard procedure for reinforced concrete structures under repeated loading conditions [25]. A one-way sinusoidal displacement history was introduced at a constant frequency of 0.2 Hz, with unloading to zero displacement after each loading cycle. The displacement amplitude was gradually increased from about 2 mm to 120 mm, allowing analysis of the response from the elastic state to failure. Because no load reversal occurred during the experiment, the loading procedure can be considered one-way repeated loading. This type of loading is typical for reinforced concrete structural elements primarily under repeated gravity loads, such as continuous beam floors, bridge beams, and parking structures under service loads. However, because this test involves no load reversal, the proposed loading procedure cannot capture response mechanisms driven by fully reversed cycles, such as tension-compression alternations, cyclic deterioration from load reversal, and hysteresis during earthquakes. Thus, the results of this research apply only to gravity loading cases and cannot be used for seismic load applications.

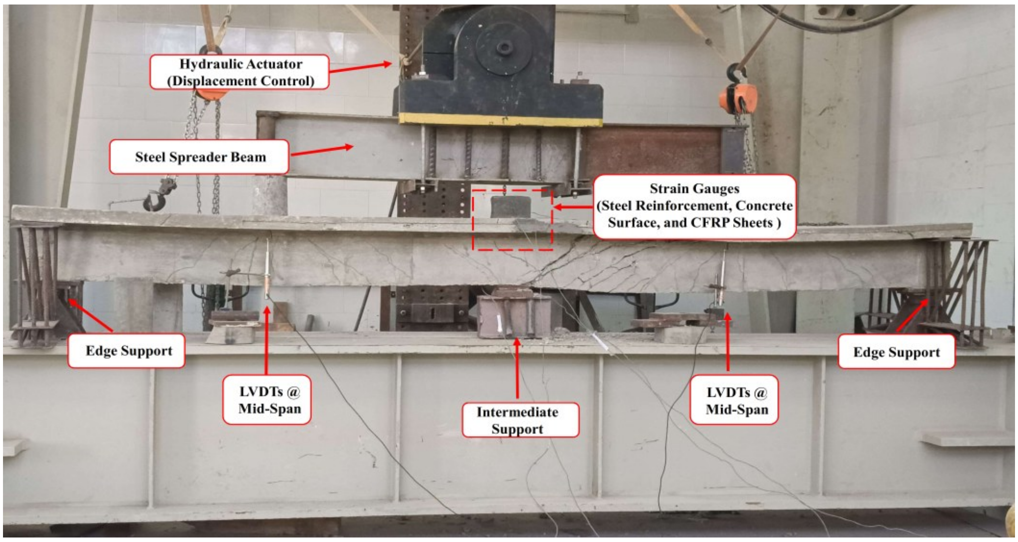

Figure 4. Experimental setup, LVDT layout, and instrumentation of the tested beams.

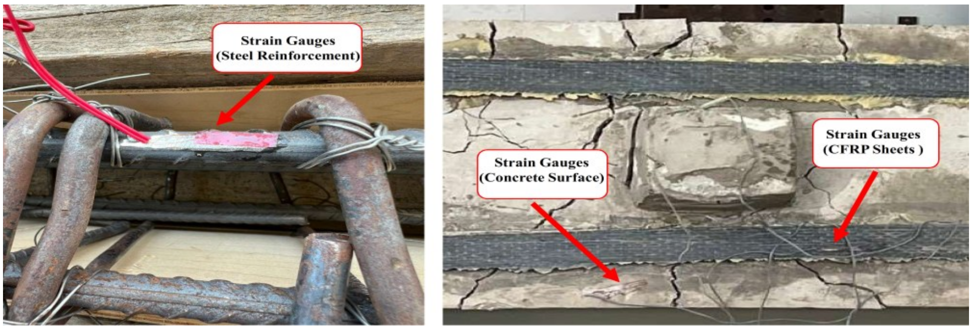

Figure 5. Strain gauge layout in the negative moment region above the intermediate support.

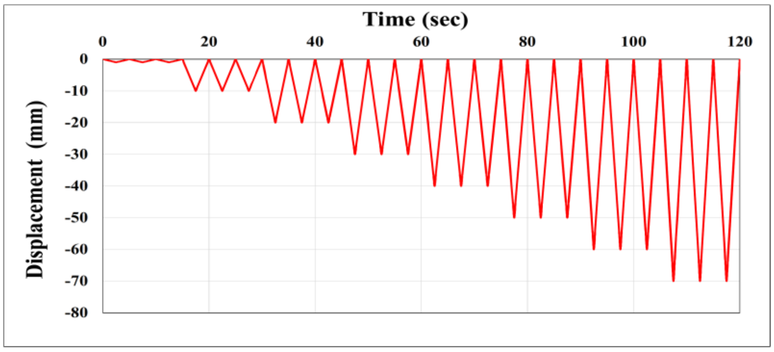

Figure 6. Displacement-controlled repeated loading protocol adopted in this study.

3. Experimental Results and Discussion

3.1. Global Structural Response under Repeated Loading

The load-displacement responses shown in Figure 7 exhibited nonlinear behavior characterized by progressive cracking, residual deformation accumulation, and widening of the hysteresis loop as the displacement amplitude rises, indicating the gradual shift from elastic to inelastic behavior.

The ductility ratio μ was defined as $\mu = \Delta u/\Delta y$, where the yield displacement Δy refers to the onset of yielding of the top longitudinal reinforcement at the intermediate support ($\varepsilon y \approx$

0.00285). The ultimate displacement Δu was considered as the maximum displacement achieved before any significant strength degradation occurs or when the test is terminated. Although the yield criterion is local, this approach was applied equally to all specimens to ensure consistency.

Parameters that describe the response of the specimens are presented in Table 3. For the control specimen (B-M-CON), the peak force was 448.25 kN, while the ultimate displacement was 32.3 mm and the ductility ratio was 2.7. Adding a CFRP layer increased the peak load by 16% (519 kN), with a marginal ductility increase to 2.9. The low-reinforcement specimens have limited load capacity but high deformation capacity, with ductility ratios of 3.9, 4.6, and 4.8 for the B-L-SL, B-L-DL, and B-L-(DL+D) specimens, respectively. The hybrid-strengthening scheme resulted in the best deformation capacity because of an improved crack pattern and less strain concentration around the intermediate support. Overall, the relationship between strength and ductility is evident: higher reinforcement leads to higher load capacity, whereas lower reinforcement and CFRP strengthening increase deformation capacity.

These findings agree with the repeated-loading results reported by Fathuldeen and Qissab [20] and Wang et al. [21], who also observed that CFRP strengthening increases the load-bearing capacity of RC beams but changes the deformation capacity because of increased structural rigidity. In the current tests on continuous beams, the effect depends not only on structural rigidity but also on the amount of reinforcement and the CFRP configuration pattern.

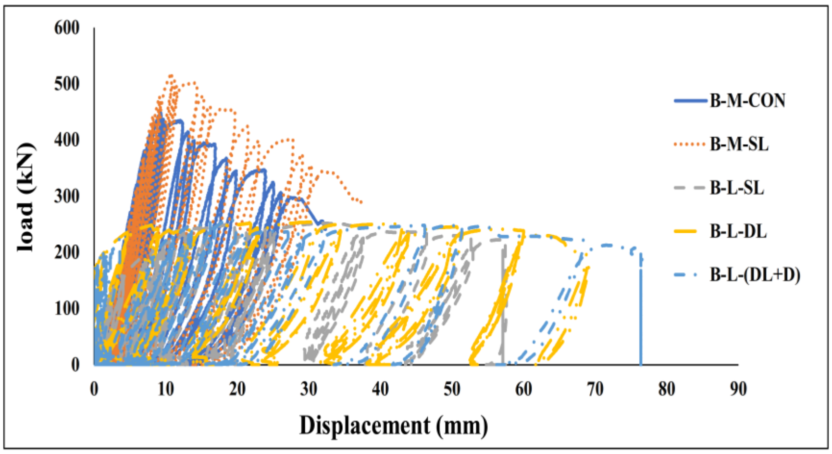

Figure 7. Load-displacement loops of the tested continuous RC beams.

Table 3. Summary of repeated loading response and displacement ductility parameters of tested specimens

Specimen	Peak Load (kN)	Δu (mm)	Δy (mm)	μ	MRI	Failure Mode
B-M-CON	448.25	32.3	12	2.7	0.57	Ductile flexural
B-M-SL	519	37.5	13	2.9	0.55	Flexural (delayed cracking)
B-L-SL	252	54.4	14	3.9	0.53	Flexural (wide cracks)
B-L-DL	254	69.1	15	4.6	0.31	Controlled flexural
B-L-(DL+D)	260	76.7	16	4.8	0.34	Flexural–shear interaction

3.2. Energy Dissipation and Stiffness Degradation

To investigate the behavior under repeated loading, the parameters of cumulative energy dissipation, residual displacement, and normalized stiffness degradation were studied. Cumulative energy dissipation was calculated as the area inside the load-displacement loops, while residual displacement and normalized stiffness were used to quantify deformation irreversibility and stiffness degradation. Table 4 summarizes the results, and Figure 8 shows the stiffness degradation curves.

Table 4. Quantitative repeated loading performance indicators of tested specimens.

Specimen	Cumulative Energy Dissipation (kN.mm)	Residual Displacement (mm)
B-M-CON	82675	14.15
B-M-SL	93155	16.28
B-L-SL	89943	41.19
B-L-DL	105425	55.10
B-L-(DL+D)	109725	61.25

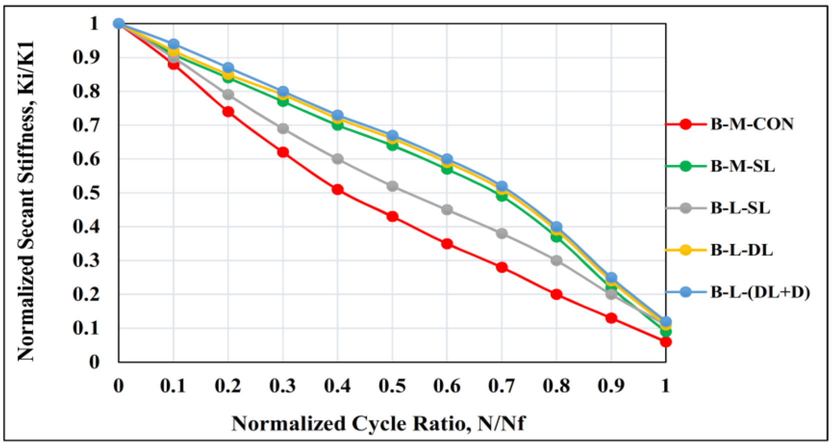

Figure 8. Normalized stiffness degradation behavior of tested continuous RC beams

The results show that CFRP reinforcement improves repeated-loading behavior by increasing energy dissipation capability, deformability, and stiffness retention. Compared with the control sample (B-M-CON), sample B-M-SL had higher cumulative energy dissipation and better stability during loading-unloading cycles. For the low-reinforcement series, significantly larger residual displacements were observed, indicating higher deformability. In this series, as the CFRP reinforcement levels increased progressively, energy dissipation capability and stiffness retention improved; hence, samples B-L-DL and B-L-(DL+D) performed better than sample B-L-SL.

From the stiffness degradation curves, all samples show decreasing stiffness due to cracking and inelastic damage accumulation. However, CFRP-reinforced samples retained a higher percentage of initial stiffness than the control sample. B-L-(DL+D) showed the best overall performance among all samples because it had the highest cumulative energy dissipation, the largest residual displacements, and the most stable stiffness development under repeated loading.

Fathuldeen and Qissab [20] and Wang et al. [21] reported similar results on progressive stiffness degradation under repeated loads. These results reveal that externally applied CFRP prevents cracks from spreading, consistent with results on stiffness maintenance in continuous beams, particularly when reinforced with CFRP.

3.3. Crack Development and Failure Modes

The crack patterns and failure modes shown in Figure 9 were generally consistent with the observed repeated loading response.

Figure 9. Crack patterns and failure modes of the tested continuous RC beam specimens.

Cracking initiated in the tension zones at locations of maximum bending moments, primarily near the intermediate support region, and progressively propagated with increasing displacement amplitudes. The test specimen B-M-CON had relatively quick crack localization and larger crack openings, indicating concentrated damage development. In contrast, the CFRP-strengthened specimens showed improved crack control, characterized by delayed crack propagation, reduced crack widths, and a more distributed crack pattern.

The influence of CFRP strengthening was particularly evident in the low-reinforcement series. Specimen B-L-SL developed wider and more localized cracks, whereas specimens B-L-DL and B-L-(DL+D) exhibited more uniform crack distribution and slower damage progression. The hybrid-strengthening configuration B-L-(DL+D) showed the most favorable crack pattern, with finer, more evenly distributed cracks throughout the critical region. Overall, CFRP strengthening reduced damage localization and promoted a more distributed cracking response, contributing to improved repeated loading stability and a more gradual failure process.

Crack behaviors found in the present investigation have been confirmed by previous studies by El-Saikaly and Chaallal [18] and Tanarslan and Altin [19], which show that CFRP reinforcement can delay crack growth and minimize crack widths. The present investigation shows that these beneficial effects were more noticeable around the intermediate supports.

3.4. Reinforcement Strain and Inelastic Behavior

The strain response of the longitudinal reinforcement at the intermediate support was used to determine the development of inelastic behavior under repeated loadings. Main parameters of strains are shown in Table 5. Steel strains increased approximately linearly during the initial loading stages and remained below the yield strain ($\varepsilon y \approx 0.00285$). As the displacement amplitude increased, yielding occurred progressively later with increasing CFRP strengthening level. The control specimen (B-M-CON) yielded at approximately 12 mm, whereas the yield displacement increased to 13, 14, 15, and 16 mm for specimens B-M-SL, B-L-SL, B-L-DL, and B-L-(DL+D), respectively. CFRP-strengthened specimens also developed higher peak and ultimate strain values, indicating improved deformation capacity and a more stable inelastic response.

Specimen B-L-(DL+D) has the most uniform strain development among all tested specimens. This indicates more evenly distributed stresses in the critical negative moment zone. Therefore, one can conclude that CFRP strengthening delays yielding and promotes more uniform inelastic behavior development.

Since strain measurements were limited to the intermediate support region, the observed behavior is interpreted as reduced strain localization rather than direct evidence of plastic hinge relocation. This interpretation is consistent with the crack development and moment redistribution results presented in the following sections.

This delay in reinforcement yielding is consistent with the findings of Akbarzadeh and Maghsoudi [14], who found that CFRP wrapping changes the strain pattern and improves the deformation properties of continuously supported RC beams. Similarly, Fathuldeen and Qissab [20] found the same effect in repeated loading cases, where CFRP wrapping delays the structure's inelastic response. Current findings show that hybrid strengthening provides a more balanced strain distribution around the negative moment zone.

Table 5. Reinforcement strain parameters of tested RC beam specimens

Specimen	Yield Strain (εy)	Δy, steel (mm)	Peak Strain (ε_{max})	Ultimate Strain (εu)
B-M-CON	0.00285	12	0.011	0.012
B-M-SL	0.00285	13	0.013	0.014
B-L-SL	0.00285	14	0.014	0.015
B-L-DL	0.00285	15	0.015	0.016
B-L-(DL+D)	0.00285	16	0.016	0.017

3.5. Moment Redistribution Behavior

The moment redistribution behavior of the tested continuous RC beams was evaluated using the measured support reactions shown in Figure 10, bending moment distributions shown in Figure 11, and the moment redistribution index (MRI) summarized in Table 3. The experimentally measured support moments (M_{exp}) were determined from the recorded reactions using static equilibrium, while the corresponding elastic moments ($M_{elastic}$) were obtained from linear elastic analysis. The MRI was calculated using Equation (1).

$$MRI = \frac{M_{elastic} - M_{exp}}{M_{elastic}} \quad (1)$$

where M_{exp} is the experimentally measured support moment, and $M_{elastic}$ is the corresponding elastic support moment. Higher MRI values indicate a greater reduction in the negative support moment relative to the elastic prediction.

The load-reaction and moment distribution analyses show that CFRP reinforcement changes the behavior of moment distribution and force redistribution in continuous beams. Specimen B-M-CON produced the maximum support moment value (approximately 224 kN·m), with an MRI value of 0.57, indicating a high value of moment redistribution, even though the ductility of this specimen was rather low (μ = 2.7). For the strengthened specimens, the support moments varied approximately within 126- 130 kN·m, while MRI values varied between 0.31 and 0.53, reflecting the influence of CFRP-induced stiffness enhancement on support moment development.

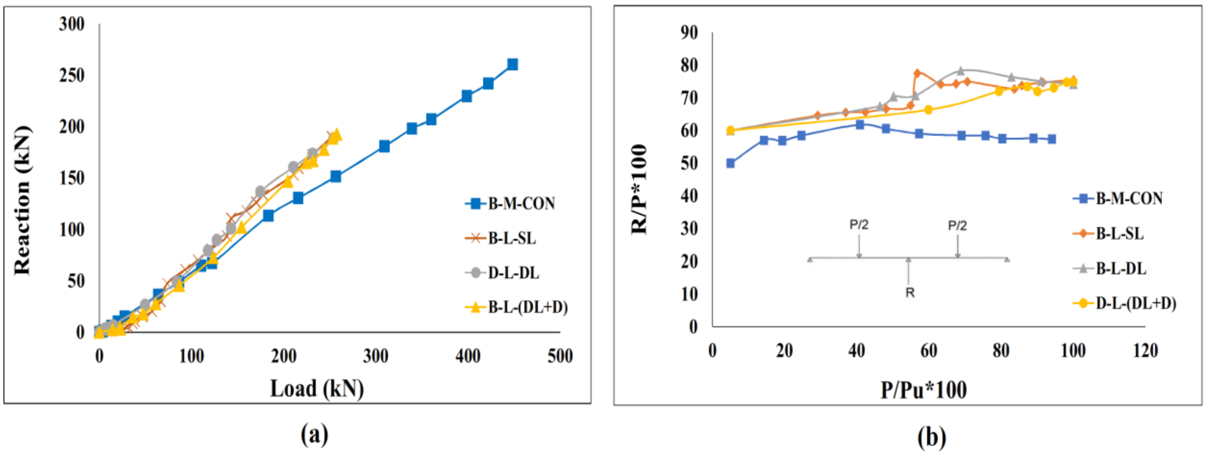

Figure 10. Load-reaction relationships of the tested continuous RC beam specimens: (a) load-reaction curves; (b) normalized load–reaction curves illustrating moment redistribution behaviour.

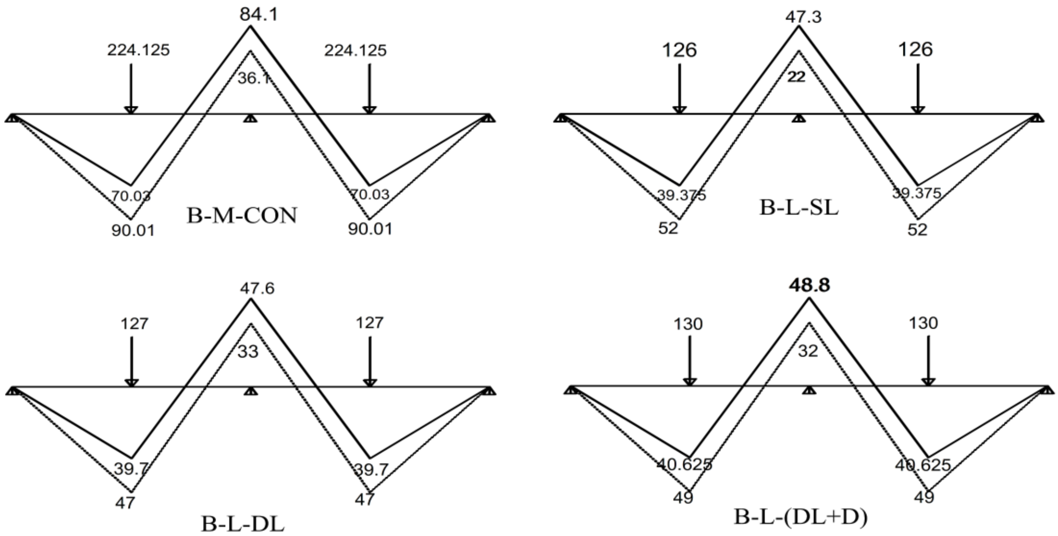

Figure 11. Bending moment distributions along the beam length for the tested beams.

Specimen B-L-SL showed the highest MRI value (0.53) among the strengthened specimens, whereas specimens B-L-DL and B-L-(DL+D) showed smaller MRI values of approximately 0.31 and 0.34, respectively, with increased beam ductility. These findings indicate a balance between rotational capacity and stiffness development, which affects moment redistribution. While CFRP strengthening improved crack control, strain distribution, and repeated-loading performance, higher strengthening levels tended to reduce redistribution efficiency by increasing local stiffness near the intermediate support. Overall, the results indicate that moment redistribution in CFRP-strengthened continuous RC beams depends on the interaction between stiffness enhancement and deformation capacity. Therefore, redistribution behavior must be considered in addition to the increase in strength.

The measured redistribution behavior agrees with previous studies highlighting the sensitivity of continuous RC beams to stiffness variation and rotational capacity. Ashour et al. [15] and El-Ghandour et al. [16] showed that CFRP strengthening affects moment redistribution in continuous beams through changes in flexural stiffness and deformation capacity. The present study observed similar behavior: higher CFRP strengthening improved strength and crack control but reduced redistribution efficiency due to increased local stiffness.

4. NUMERICAL MODELING AND VALIDATION

The experimental program provided valuable insight into the repeated-loading behavior of CFRP-strengthened continuous RC beams; however, its scope was limited by the cost and complexity of full-scale testing. Accordingly, a three-dimensional nonlinear finite element (FE) model was developed in ABAQUS and validated using the experimental results. The model was intended to reproduce the global structural response and the associated damage mechanisms governing stiffness degradation, strain development, and moment redistribution under repeated loading.

4.1. Finite Element Modeling

A three-dimensional nonlinear FE model was developed to simulate the tested continuous RC T-beams under displacement-controlled repeated loading. The model replicated the experimental geometry, reinforcement detailing, support conditions, and CFRP strengthening layouts, as shown in Figure 12.

Concrete was modeled using 8-node reduced-integration solid elements (C3D8R), with mesh refinement in the area of negative moment near the intermediate support. The reinforcing steel was represented with embedded beam elements (B31), assuming full bonding between steel and concrete. This assumption was considered appropriate because the experimental tests showed no evidence of reinforcement slip or bond-related failure, indicating that the global response was governed by flexural behavior rather than bond deterioration. The CFRP strips were modeled using 4-node shell elements (S4R) with orthotropic elasticity and fiber orientation according to the strengthening scheme. The interaction of CFRP with the concrete was simulated using tie constraints, while CFRP debonding was not considered because no premature debonding or rupture was observed experimentally.

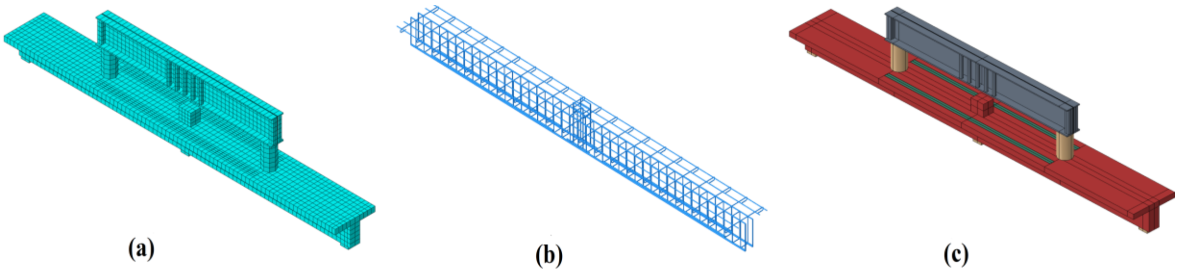

Figure 12. Finite element model of the tested continuous RC beam system: (a) concrete mesh; (b) embedded reinforcement; (c) CFRP strengthening.

Table 6. CDP parameters adopted in the FE model

Parameter	ψ	ε	f_{b0}/f_{c0}	K_c	Viscosity parameter
Value	36°	0.10	1.16	0.667	0.0005

The Concrete Damage Plasticity (CDP) material model in ABAQUS captured the nonlinear response of concrete. The parameters used in the simulation, listed in Table 6, were calibrated based on material characteristics obtained from test results and the literature. The tensile and compressive behavior of concrete included damage accumulation and stiffness reduction, whereas steel reinforcement was modeled using an elastic-plastic constitutive model with isotropic hardening. The simulation loading sequence followed the experimentally

https://doi.org/10.31436/iiumej.v27i3.4517

obtained displacement-controlled method, including unloading-reloading cycles with increasing displacement steps. The simulation applied loads using rigid loading plates to ensure uniform load transfer.

4.2. Model Verification

In this work, the FE analysis was validated experimentally based on the structure's global response, strain development in reinforcements, reactions, and progressive damage. Figure 13 compares the numerical and experimental load-displacement responses, while Table 7 compares peak load and ultimate displacement.

The numerical model can predict the entire repeated-loading process, including initial stiffness, yielding, peak load, stiffness reduction, residual displacements, and unloading-reloading behavior. Peak load predictions showed a 2.6%- 11.5% difference compared to experimental peak loads, whereas ultimate displacement showed differences of 7.6%- 11.6%. Mean errors for peak load and ultimate displacement were 7.5% and 9.1%, respectively. Initial stiffness was underpredicted in some experiments, which could be due to the assumption of perfect bonding and no existing microcracks in the numerical simulation.

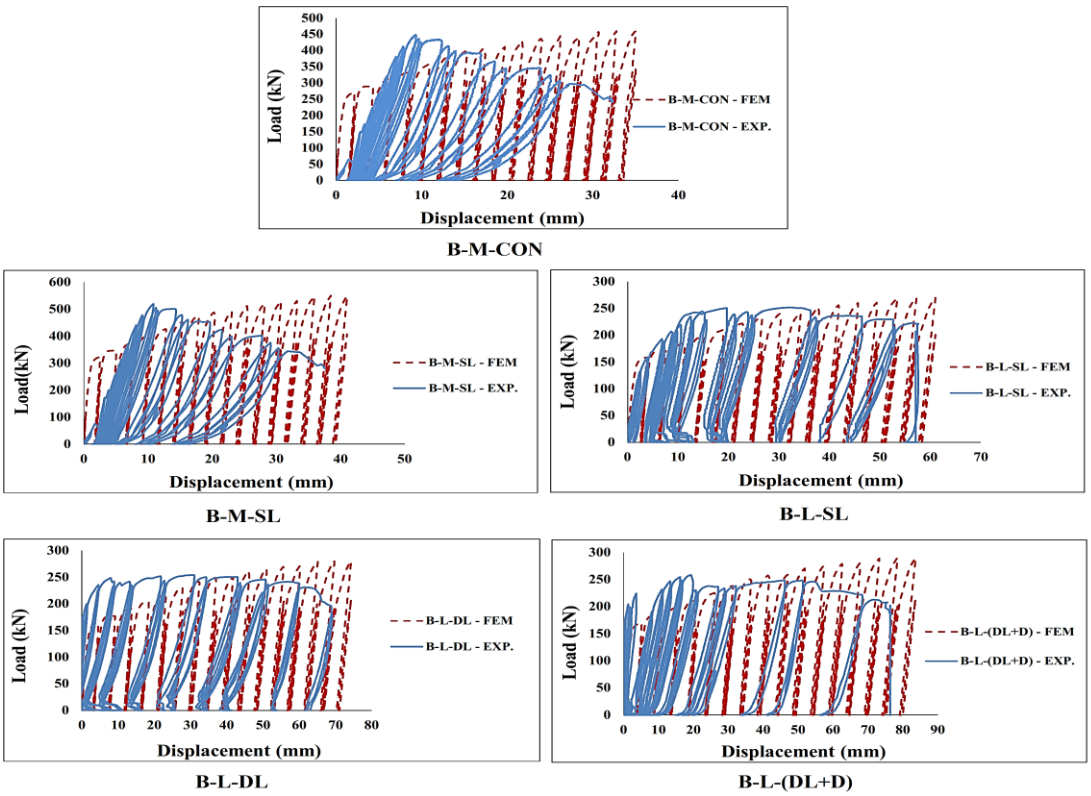

Figure 13. Comparison of experimental and numerical (FEM) load-displacement loops for all beams.

The FE analysis predicted the experimentally observed trends in reinforcement strain evolution and reaction progression, namely delayed yielding and reduced strain localization in CFRP-strengthened beam specimens. Moreover, the tensile damage contours computed based on the CDP model shown in Figure 14 showed good correspondence to the actual cracking, properly detecting regions with increased damage concentrations near the intermediate support point. Although the CDP model damage contours represent material deterioration rather than cracks, the simulation adequately captured the experimentally observed reduction in damage localization and improved cracking behavior caused by CFRP strengthening.

Table 7. Comparison between experimental and FE results

Specimen	$P_{max\text{-}EXP}$ (kN)	$P_{max\text{-}FEM}$ (kN)	Error	$\Delta u_{\text{-}EXP}$ (mm)	$\Delta u_{\text{-}FEM}$ (mm)	Error
B-M-CON	448.25	460	2.6%	32.5	35.0	8.4%
B-M-SL	519.0	550	6.0%	37.5	41.0	9.2%
B-L-SL	252.0	270	7.2%	54.4	60.7	11.6%
B-L-DL	254.0	280	10.2%	69.1	74.3	7.6%
B-L-(DL+D)	260.0	290	11.5%	76.7	83.6	8.9%
Mean Error	—	—	7.5%	—	—	9.1%

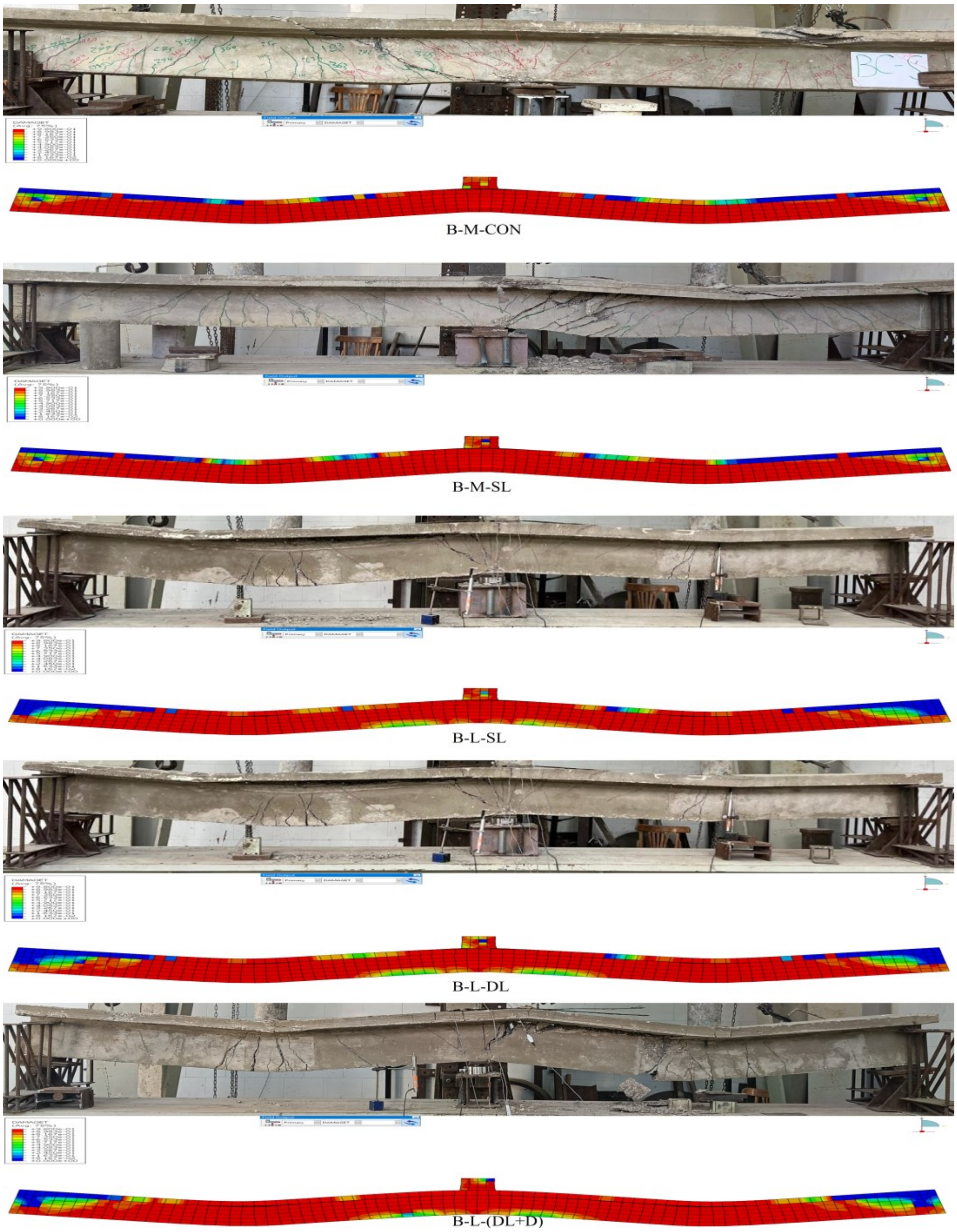

Figure 14. Comparison of numerical damage contours with experimental crack patterns for the tested beams.

Overall, the agreement between the numerical predictions and experimental observations demonstrates that the developed FE model provides a reliable framework for simulating the repeated-loading behavior of CFRP-strengthened continuous RC beams within the investigated parameter range. Nevertheless, the adopted perfect-bond assumption and the smeared-crack representation of concrete damage need to be considered when interpreting localized cracking and damage patterns.

5. PARAMETRIC STUDY AND DISCUSSION

After validating the FE model, a parametric study was performed to examine the effect of various structural, material, and strengthening parameters on the repeated-loading response of CFRP-strengthened RC continuous beams. The validated model enabled the manipulation of the investigated parameters while keeping the same geometric characteristics, boundary conditions, and loading sequence.

Specimen B-L-SL was adopted as the reference model because it exhibited a balanced combination of strength, deformation capacity, and repeated-loading performance. The investigated parameters, summarized in Table 8, included the negative reinforcement ratio (ρ_n), concrete compressive strength (F_{cu}), span-to-depth ratio (L/d), CFRP reinforcement ratio (ρ_f), CFRP length ratio (Lf/L), loading frequency (Δ), and steel yield strength (F_y). The CFRP reinforcement ratio (ρf) was calculated as the ratio of the total CFRP cross-sectional area to the concrete web cross-sectional area, considering the number of CFRP layers and the thickness of each layer, as expressed in Equation (2).

$$\rho_f = \frac{n_f * b_f * t_f}{b_w * d} \tag{2}$$

where, n_f is the number of CFRP layers, b_f is the CFRP strip width, t_f is the thickness of one CFRP layer (0.164 mm), b_w is the beam web width, and d is the effective depth of the beam. The CFRP reinforcement ratio was varied by changing the number of CFRP layers (one to five layers), while maintaining a constant CFRP sheet thickness of 0.164 mm per layer.

Table 8. Variables considered in the parametric investigation (baseline: specimen B-L-SL)

Parameter	Levels Considered	Mechanical Role
Negative reinforcement ratio (ρ_n)	0.46, 0.66, 1.20 %	Governs hogging moment capacity, crack control, and stiffness degradation at supports
Concrete compressive strength (F_{cu})	30, 40, 50 MPa	Controls compression zone behavior, ductility, and failure mode
Span-to-depth ratio (L/d)	12, 15, 18	Influences flexural stiffness, deformation capacity, and moment redistribution
CFRP reinforcement ratio (ρ_f)	0.024, 0.048, 0.072, 0.096, 0.12 % (corresponding to one to five CFRP layers with a constant thickness of 0.164 mm per layer)	Enhances flexural capacity, stiffness, and repeated loading performance
CFRP length ratio (L_f/L)	0.25, 0.50, 0.75, 1.00	Affects stress distribution and deboning resistance
Loading frequency (Δ)	0.1, 0.2, 0.3 Hz	Influences rate effects, energy dissipation, and damage accumulation
Steel yield strength (F_y)	350, 570, 650 MPa	Controls yielding behavior, ductility, and energy dissipation

This study used a one-variable-at-a-time approach. In this approach, each parameter is varied individually while the rest remain constant. The study focused on capacity under repeated loads, displacement capacity, ductility, stiffness degradation, and overall behavior. This will be discussed in the following section.

5.1. Influence of Structural and Material Parameters

Figure 15 presents the influence of the investigated structural and material parameters on the repeated-loading response. Increasing the negative reinforcement ratio (ρ_n) and steel yield strength (F_y) increased load-carrying capacity and stiffness by improving flexural resistance in the negative moment region. However, the associated increase in stiffness reduced deformation capacity and ductility by limiting curvature development and rotational demand.

The span-to-depth ratio (L/d) exhibited an opposite trend. Lower L/d ratios increased stiffness and load resistance, whereas larger ratios promoted greater deformation capacity and ductility at the expense of a moderate strength reduction. Increasing the concrete compressive strength (F_{cu}) also improved load capacity by delaying compressive damage development, although its influence on deformation behavior was less pronounced than that of reinforcement-related parameters.

Overall, the results demonstrate a clear trade-off between strength and deformation capacity. Parameters that enhance stiffness and flexural resistance generally increase load capacity but may reduce ductility and rotational capacity. Therefore, the performance of CFRP-strengthened continuous beams under repeated loading should be assessed by considering both strength and deformation characteristics, not strength enhancement alone.

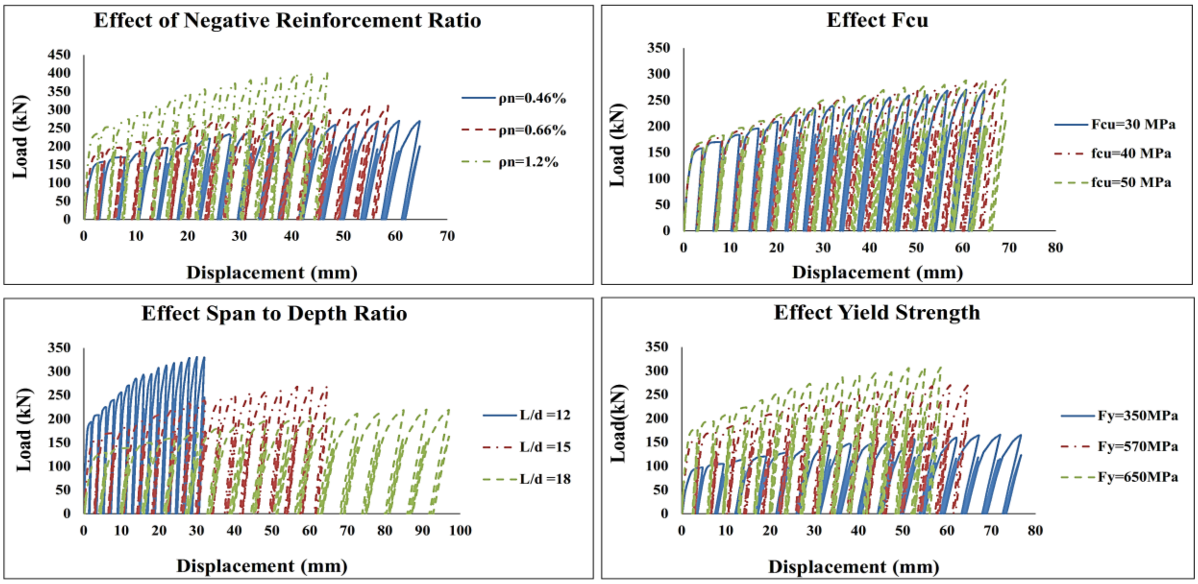

Figure 15. Influence of key structural and material parameters on the load-displacement loops of the tested beams.

5.2. Influence of CFRP Strengthening Parameters

Figure 16 shows the effect of CFRP strengthening parameters on repeated-loading behavior. Increasing the CFRP reinforcement ratio (ρ_f) increased load capacity, crack control, and stiffness. However, excessive strengthening reduced deformation capacity and rotation requirement, suggesting stiffness-controlled behavior.

The CFRP strengthening ratio (Lf/L) affected structural behavior by increasing stress transfer along the reinforced region and reducing stress concentrations at the CFRP ends. Compared with increasing the CFRP ratio alone, increasing the CFRP length provided more consistent results, with small increases in load capacity and limited decreases in deformation capacity.

Overall, the results indicate that the effectiveness of CFRP strengthening depends not only on the amount of CFRP reinforcement but also on its distribution along the beam. Therefore, strengthening design should balance stiffness enhancement and crack control with adequate deformation capacity to ensure stable behavior under repeated loading.

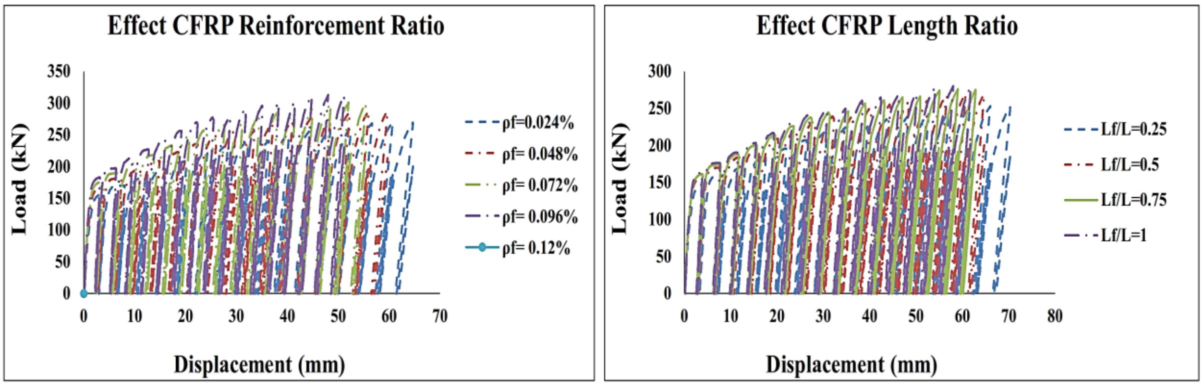

Figure 16. Influence of CFRP strengthening parameters on the load–displacement loops of the tested beams.

5.3. Influence of Loading Conditions

Figure 17 illustrates the influence of loading frequency on repeated-loading behavior. In the investigated quasi-static frequency range (0.1–0.3 Hz), the variation in load-bearing capacity and displacement behavior was minimal, suggesting no sensitivity to loading frequency. This shows that inertia and rate sensitivity are insignificant in the selected frequency range. As a result, the structure's response depends mainly on the beam geometry and the CFRP strengthening parameters.

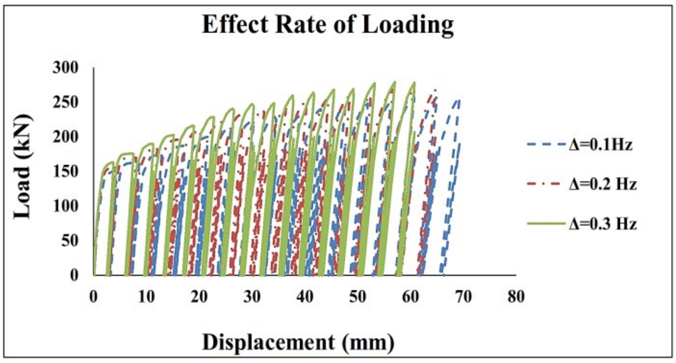

Figure 17. Influence of loading frequency on the load-displacement loops of the tested beams.

5.4. Integrated Discussion of Repeated Loading Behavior and Moment Redistribution

Both the experimental and numerical results suggest that the repeated-loading response of continuously reinforced concrete beams strengthened with CFRP is governed by the interaction among the following factors: stiffness development, damage accumulation, deformation capacity, and rotation compatibility. CFRP strengthening of RC beams typically enhances crack development, delays stiffness reduction, and reduces damage localization, leading to more stable behavior under repeated loads.

The moment redistribution process depends significantly on the relationship between the stiffness and rotation capacity. High values of parameters that increase stiffness, such as high reinforcement ratios, high steel yield strength, and high CFRP ratios, improve load-carrying capacity but reduce deformation capacity and redistribution efficiency. Parameters that increase flexibility and stress uniformity, such as span-to-depth ratio and CFRP layout, improve deformation capacity and redistribution.

The results show that repeated-loading performance and moment redistribution cannot be assessed solely by strength enhancement. Effective strengthening strategies should balance load capacity, crack control, deformation capacity, and redistribution capability to ensure stable performance under repeated loading conditions.

6. Simplified Load Capacity Prediction

6.1. Development of the Predictive Model

To provide a practical tool for preliminary estimation of the load capacity of CFRP-strengthened continuous RC beams, a simplified prediction equation was developed based on the validated FE database. The database consisted of 18 numerical cases, including the reference model and 17 parametric variations covering the ranges listed in Table 9. The investigated variables were the negative reinforcement ratio (ρ_n), concrete compressive strength (F_{cu}), span-to-depth ratio (L/d), CFRP reinforcement ratio (ρ_f), CFRP length ratio (L_f/L), loading frequency (Δ), and steel yield strength (F_y). A nonlinear regression analysis based on a multiplicative power-law formulation was performed, resulting in Eq. (3).

$$P_{equ} = 114.27{\rho_n}^{0.425}{F_{cu}}^{0.159}\left(\frac{L}{d}\right)^{-0.977}{\rho_f}^{0.111}\left(\frac{Lf}{L}\right)^{0.072}\Delta^{0.067}{F_y}^{0.997} \quad (3)$$

The obtained exponents indicate that steel yield strength and span-to-depth ratio have the greatest influence on load capacity within the investigated parameter ranges, whereas the remaining parameters contribute to a lesser extent. The proposed equation is intended as a simplified engineering estimation tool and should therefore be applied only within the parameter ranges considered in the present study.

6.2. Model Validation

The proposed equation was evaluated first against the FE database used for its development. As shown in Table 9, the model showed excellent agreement, with a mean predicted-to-FE ratio of 0.999 and a coefficient of variation (COV) of 0.8%.

To assess the model's applicability beyond the calibration dataset, we performed independent validation using experimental results reported by El-Ghandour et al. [16] and Ashour et al. [15]. The validation results are summarized in Tables 10 and 11. For the El-Ghandour et al. [16] dataset, the predicted-to-experimental ratios ranged from 0.953 to 1.036, with a mean of 0.988 and a COV of 3.2%. For the Ashour et al. [15] dataset, the ratios ranged from 0.91 to 1.05, with a mean value of 0.95 and a COV of 5.0%. As illustrated in Figure 18, most predictions were located close to the line of equality, indicating satisfactory agreement with the experimental observations.

This proposed formulation can be used for continuous CFRP-strengthened RC beams subjected to repeated loads, where gravity is the main load component, within the parameter range tested in this study. The applicability range includes beams with similar continuous beam configurations, flexural strengthening using CFRP sheets, reinforcement ratios, concrete compressive strengths, CFRP reinforcement ratios, CFRP length ratios, steel grades, and loading frequencies represented by the developed FE database and validation datasets. Therefore, the equation is intended as a simplified engineering prediction tool for preliminary load-capacity estimation rather than a universal design equation for all CFRP-strengthened RC beams.

Table 9. Validation of the proposed model against FE results

Case	Varied Parameter	Value	P_{FE} (kN)	P_{Eq} (kN)	P_{Eq} / P_{FE}
Ref	—	—	270	267.8	0.992
1	ρ_n	0.66%	312	312.2	1.001
2	ρ_n	1.20%	403	402.5	0.999
3	Fcu	40 MPa	282	280.3	0.994
4	F_{cu}	50 MPa	290	290.5	1.002
5	L/d	12	331	333.1	1.006
6	L/d	18	220	224.1	1.019
7	ρ_f	0.048%	288	289.2	1.004
8	ρ_f	0.072%	301	302.6	1.005
9	ρ_f	0.096%	313	312.4	0.998
10	ρ_f	0.12%	322	320.3	0.995
11	L_f/L	0.25	253	254.7	1.007
12	L_f/L	0.75	276	275.7	0.999
13	L_f/L	1.00	280	281.5	1.005
14	Δ	0.1 Hz	258	255.5	0.990
15	Δ	0.3 Hz	279	275.2	0.986
16	F_y	350 MPa	166	164.6	0.992
17	F_y	650 MPa	308	305.3	0.991
Mean	—	—	—	—	**0.999**
COV	—	—	—	—	**0.8%**

Table 10. Validation of the proposed model against experimental results reported by El-Ghandour et al. (2004).

Beam	P_{exp} (kN)	P_{eq} (kN)	P_{eq} / P_{exp}
B1	170	162	0.953
B2	235	228	0.970
B3	255	262	1.027
B4	195	188	0.964
B5	250	244	0.976
B6	280	290	1.036
Mean	—	—	0.988
COV	—	—	3.2%

Table 11. Validation of the proposed model against experimental results reported by Ashour et al. (2004).

Beam	P_{exp} (kN)	P_{eq} (kN)	P_{eq} / P_{exp}
H1	138.0	145	1.05
H3	172.9	160	0.93
S4	170.5	155	0.91
E2	178.6	170	0.95
E3	207.0	190	0.92
E4	231.4	215	0.93
E5	174.6	165	0.95
Mean	—	—	0.95
COV	—	—	5.0%

Despite the successful results achieved in this validation process, a few limitations must be considered when using this equation. The formulation was based on a one-factor-at-a-time parametric database, so it does not account for possible interactions between parameters. This equation also does not account for CFRP debonding, bond slip, different failure modes, or fully reversed cyclic loading.

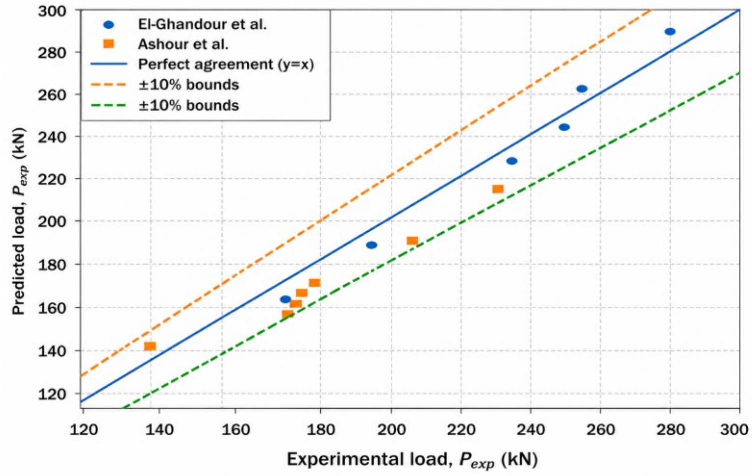

Figure 18. Comparison between predicted and experimental loads for the independent datasets reported by El-Ghandour et al. [16] and Ashour et al. [15]

Overall, the proposed formulation provides a simple and physically interpretable method for estimating the load capacity of CFRP-strengthened continuous RC beams subjected to gravity-dominated repeated loading. Within the identified applicability range, the equation provides reliable predictions; however, further validation using larger databases and broader parameter combinations is recommended to enhance its generalization and applicability.

7. CONCLUSIONS AND FUTURE WORK

This study investigated the repeated-loading response and moment-redistribution capacity of CFRP-strengthened continuous RC T-beams based on experimental tests and nonlinear FE modeling. Results showed that CFRP strengthening increases repeated-loading resistance by providing higher load capacity, better energy absorption, delayed stiffness loss, and more uniformly distributed crack and deformation patterns. The strengthening configuration strongly affects the structure's performance under repeated loading, with the hybrid longitudinal-diagonal CFRP scheme showing the most stable response.

Furthermore, the CFRP strengthening delays yielding of reinforcing bars and reduces strain concentrations in the negative moment zone. However, the influence of CFRP strengthening on moment redistribution is determined by the balance between stiffness improvement and rotational ability of the section. Although CFRP improves crack and damage distribution, excessive stiffening reduces moment-redistribution efficiency, implying that increased structural strength does not always lead to more efficient redistribution.

The parametric study revealed a trade-off between strength and ductility. The reinforcement ratio and yield strength increase the section's load capacity but reduce its deformation capacity, whereas a higher span-to-depth ratio provides ductility and moment redistribution at the cost of reduced load capacity. Lengthening the CFRP improves stress distribution and repeated-loading behavior; however, an excessive CFRP ratio decreases ductility because of increased stiffness. Higher concrete compressive strength increases the compressive stability, whereas loading frequency has little effect within the analyzed quasi-static range.

The validated FE model reproduced the experimental response with satisfactory accuracy and was used to generate a numerical database for developing a simplified load-capacity prediction model. Overall, the results indicate that effective strengthening design should balance strength enhancement, deformation capacity, rotational compatibility, and moment redistribution rather than maximizing stiffness alone.

Future research should extend the proposed framework to fully reversed cyclic and seismic loading conditions while incorporating bond-slip effects, CFRP debonding behavior, and broader experimental validation covering a wider range of beam geometries and strengthening configurations.

REFERENCES

[1] Aydogan MS, Aydemir C, Arslan G. (2024) Moment redistribution in continuous reinforced concrete beams: Experimental study and analytical investigation. Structures, 63: 106440. https://doi.org/10.1016/j.istruc.2024.106440

[2] Li L, Li B, Zheng W. (2024) Moment Redistribution in UHPC Continuous Beams Reinforced with High-Strength Steel Bars: Numerical Investigation and Prediction Model. Buildings, 14(1):149. https://doi.org/10.3390/buildings14010149

[3] Qureshi HJ, Althoey MA, Alqahtani A, Hadi MA, Elhaddad MM, Mohamed MA, et al. (2022) Investigation of CFRP Reinforcement Ratio on the Flexural Capacity and Failure Mode of Plain Concrete Prisms. Materials, 15(20):7248. https://doi.org/10.3390/ma15207248

[4] Kim HG, Lee YJ, Kim KH. (2022) Cyclic flexural performance of RC beams with small circular openings in plastic hinge region. Construction and Building Materials, 321:126339. https://doi.org/10.1016/j.conbuildmat.2022.126339

[5] Jahami A, Issa CA. (2024) An Updated Review on the Effect of CFRP on Flexural Performance of Reinforced Concrete Beams. International Journal of Concrete Structures and Materials, 18(1):14. https://doi.org/10.1186/s40069-023-00651-y

[6] Suliman AKE, Jia Y, Mohammed AAA. (2021) Experimental evaluation of factors affecting the behavior of reinforced concrete beams strengthened by NSM CFRP strips. Structures, 32:632–640. https://doi.org/10.1016/j.istruc.2021.03.058

[7] Shaikh ZK, Sohoni VS. (2025) Efficacy of carbon fibre reinforced polymer (CFRP) laminates in retrofitting the damaged moment resisting RC frames. Discover Civil Engineering, 2(1):166. https://doi.org/10.1007/s44290-025-00326-5

[8] Alsuhaibani E. (2024) Optimization of Carbon Fiber-Reinforced Polymer (CFRP) Configuration for Enhanced Flexural Performance in Strengthened Concrete Beams. Buildings, 14(12):3953. https://doi.org/10.3390/buildings14123953

[9] Lou T, Lopes SMR, Lopes AV. (2014) Factors affecting moment redistribution at ultimate in continuous beams prestressed with external CFRP tendons. Composites Part B: Engineering, 66:136–146. https://doi.org/10.1016/j.compositesb.2014.05.007

[10] Kalyani G, Pannirselvam N. (2023) Experimental and numerical investigations on RC beams flexurally strengthened utilizing hybrid FRP sheets. Results in Engineering, 19:101337. https://doi.org/10.1016/j.rineng.2023.101337

[11] Yagmur E. (2026) Parametric study on the behavior of CFRP-strengthened reinforced concrete deep beams with cut circular web openings in shear spans. Scientific Reports, 16: 9414. https://doi.org/10.1038/s41598-026-40071-y

[12] Li R, Aboutaha RS. (2025) Analytical Investigation of CFRP- and Steel Plate-Strengthened RC Beams with Partially Unbonded Reinforcement. Buildings, 15(20):3665. https://doi.org/10.3390/buildings15203665

[13] Szczepański K, Kotynia R. (2024) Bending moments redistribution in two-span reinforced concrete beams reinforced with FRP bars based on collected data research. Structural Concrete, 25(2):1076–1091. https://doi.org/10.1002/suco.202300329

[14] Akbarzadeh H, Maghsoudi AA. (2010) Experimental and analytical investigation of reinforced high strength concrete continuous beams strengthened with fiber-reinforced polymer. Materials and Design, 31(3):1130–1147. https://doi.org/10.1016/j.matdes.2009.09.041

[15] Ashour AF, El-Refaie SA, Garrity SW. (2004) Flexural strengthening of RC continuous beams using CFRP laminates. Cement and Concrete Composites, 26(7):765–775. https://doi.org/10.1016/j.cemconcomp.2003.07.002

[16] El-Ghandour A, Aly H, Nasr E, Abdelrahman A. (2004) Moment redistribution in RC continuous beams strengthened in flexure by CFRP laminates. In: FRP Composites in Civil Engineering (CICE 2004):227–235. https://doi.org/10.1201/9780203970850.ch22

[17] Aiello MA, Valente L, Rizzo A. (2007) Moment redistribution in continuous reinforced concrete beams strengthened with carbon-fiber-reinforced polymer laminates. Mechanics of Composite Materials, 43(5):453–466. https://doi.org/10.1007/s11029-007-0043-x

[18] El-Saikaly G, Chaallal O. (2015) Cyclic performance of reinforced concrete T-beams strengthened in shear with fiber-reinforced polymer composites: Sheets versus laminates. Journal of Reinforced Plastics and Composites, 34(13):1040–1058. https://doi.org/10.1177/0731684415587347

[19] Tanarslan HM, Altin S. (2010) Behavior of RC T-section beams strengthened with CFRP strips, subjected to cyclic load. Materials and Structures, 43(4):529–542. https://doi.org/10.1617/s11527-009-9509-8

[20] Fathuldeen SW, Qissab MA. (2019) Behavior of RC Beams Strengthened with NSM CFRP Strips under Flexural Repeated Loading. Structural Engineering and Mechanics, 70(1):67–80. https://doi.org/10.12989/sem.2019.70.1.067

[21] Wang H, Li C, Song S, Wang Y, Meng Q, Li F. (2023) Flexural Performance of Cracked Reinforced Concrete Beams Strengthened with Prestressed CFRP Sheets under Repeated Loads. Buildings, 13(8):2115. https://doi.org/10.3390/buildings13082115

[22] ECP 203-2020. (2020) Egyptian Code for Design and Construction of Reinforced Concrete Structures. Housing and Building National Research Center (HBRC), Cairo, Egypt.

[23] BS EN 12390-3:2019. (2019) Testing Hardened Concrete-Part 3: Compressive Strength of Test Specimens. British Standards Institution.

[24] ASTM A370-22. (2022) Standard Test Methods and Definitions for Mechanical Testing of Steel Products. ASTM International.

[25] García JM, Bonett RL, Schultz AE, Carrillo J, Ledezma C. (2019) Flexural behavior of ungrouted post-tensioned concrete masonry beams with unbonded bars. Construction and Building Materials, 203:210–221. https://doi.org/10.1016/j.conbuildmat.2018.12.101